BEAM DYNAMICS DESIGN OF A SYNCHROTRON INJECTOR WITH LASER-ACCELERATED IONS

M. Z. Tuo, Q. Z. Xing, X. L. Guan, S. X. Zheng, H. J. Yao, W. Lu, P. F. Ma, X.W. Wang[†]

Key Laboratory of Particle & Radiation Imaging (Tsinghua University),

Ministry of Education, Beijing, China,

Laboratory for Advanced Radiation Sources and Application,

Tsinghua University, Beijing, China,

Department of Engineering Physics, Tsinghua University, Beijing, China

Y. Wan

Department of Physics of Complex Systems,

Weizmann Institute of Science, Rehovot, Israel

Abstract

We present, in this paper, the beam dynamics design of a linac injector with laser-accelerated carbon-ions for a medical synchrotron. In the design, the initial transverse divergence is reduced by two apertures. The beam is focused transversely through a quadrupole triplet lens downstream the apertures. The output energy spread of the extracted beam at the exit of the injector is compressed from ±6% to ±0.6% by a debuncher and a bend magnet system to meet the injection requirement for the synchrotron. By changing the width of imaging slit of the bend magnet system, the beam with energy of 4±0.024 MeV/u is extracted, and the particle number per shot and transverse emittances of the beam at the exit of the injector can be regulated through adjusting the slit height. The dynamics design can pave the way for the future concept research of the synchrotron injector.

INTRODUCTION

During the past ten years, there have been prospective researches on taking use of laser-accelerated ions to act as substitute of traditional particle sources [1-5]. Laser-accelerated ion beam has several characteristics: 1) the normalized RMS emittance can be as low as 0.01 π mm·mrad and typical transverse beam radius is 10~100 μm; 2) the beam pulse length and peak current can be less than 1 ps and up to several to tens kA, respectively; 3) the number of particles per shot can be greater than 10^{11} [6, 7]. While it has a quasi-monoenergy and repetition frequency of 10~1000 Hz, laser-accelerated ion beam has very attractive prospect in the miniaturization of tumour ion therapy facility. For instance, researches have been done in Quantum Scalpel Project by QST in Japan [2] and LIGHT project by GSI in Germany [3, 4]. Among varieties of laser-ion acceleration mechanism, Target Normal Sheath Acceleration (TNSA), in which a 1~10 μm thick target is irradiated by the ultra-intense (>10^{19} W/cm^2) short pulse laser, is one of the most stable methods to obtain tens MeV of ions [6]. However, up to now, the laser-accelerated ion beam generated by means of TNSA in the experiment generally follows an exponentially decaying energy spectrum. For synchrotron injection with laser-accelerated ion beam, in which a sufficient number of particles is required, reducing energy spread and transverse divergence of the beam from TNSA are of vital importance.

As part of concept research for a compact heavy-ion radiotherapy facility in the future, we present, in this paper, the beam dynamics design of a carbon-ion linac injector originated from laser-accelerated ions for a medical synchrotron.

INPUT BEAM PARAMETERS

In the beam dynamics design, the initial distribution of C^{6+} ions is generated by a Particle-In-Cell (PIC) simulation of a 300 TW laser bombarding on a 5 μm-thick aluminium target in 30 fs, with the mechanism of TNSA [8]. The phase space distribution and transverse profile of the produced ions are shown in Fig. 1. The six-dimensional phase space parameters of the macroparticles are then exploited for the beam dynamics design of the linac injector.
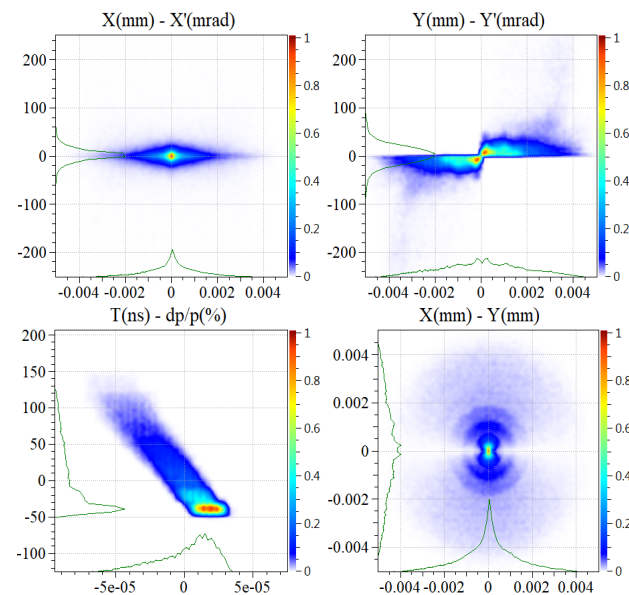

Figure 1: Phase space distribution and transverse profile of the simulated laser-accelerated carbon-ions. (2.08×10^5 macroparticles).

† wangxuewu@tsinghua.edu.cn.

As shown in Fig. 1, for a reference energy of 4 MeV/u, the energy spread of laser-accelerated C^{6+} beam ranges from -100% to 300%. Therefore, it is necessary to reduce the energy spread for injection into synchrotron. In addition, the peak current reaches up to 6 kA with the bunch length of 0.15 ps and particle number of 10^{11}, which leads to intense space charge effect. To suppress it, extension of the bunch length is required. It is also worth noting that the transverse divergence is approximately ±100 mrad，which will lead to unacceptable beam envelope growth. Hence there is great demand to control the transverse divergence by lenses and apertures.

LINAC INJECTOR LAYOUT

The linac injector is primarily designed for transportation, transverse focusing and matching, and longitudinal debunching of the laser-accelerated C^{6+} ions. The overall layout is shown in Fig. 2.
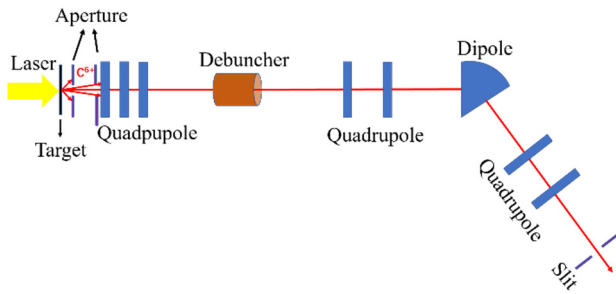

Figure 2: Schematic of the linac injector.

In Fig. 2, two apertures with variable bore diameter are adopted just downstream the target for the transverse divergence control. Then the beam is focused by a triplet quadrupole lens and transported to a debuncher.

The energy spread of the injected beam for the synchrotron is required to be within ±0.6%. The energy spread is compressed by the debuncher, and a dispersive bend magnet system which consists of a bend magnet, four quadrupole lenses and an imaging slit. To reduce the transverse dimension of the debuncher, the debuncher is arranged at the focal point of the triplet quadrupole lens, which is also the object point of the dispersive bend magnet system. The magnet system focuses the beam at the imaging point upstream the exit of the injector, where a slit is set up to control the output energy spread. To restrain transverse envelope growth, there are two quadrupole lenses placed at each end of the bend magnet.

BEAM DYNAMICS DESIGN

The research result indicates that, the space charge of laser-accelerated ions produced from TNSA is neutralized by co-moving hot electron cloud in the early phase of bunch expansion close to the target source [6, 9]. In consequence, unless external electromagnetic field is introduced, the beam can be regarded as electrically neutral. Therefore, in the dynamics simulation, the space charge effect of the C^{6+} beam is neglected from the target to the first quadrupole, while included in the rest part of the injector.

The multiparticle simulation is carried out by the Trace-Win code [10]. The particle distribution in Fig. 1 is adopted for simulation and the total number of input macroparticles is 2.08×10^5. With the distance between the two apertures of 300 mm, and bore radii of 10 mm and 11 mm, respectively, the transverse divergence at the entrance of first quadrupole is reduced to ±30 mrad, as shown in Fig. 3. The transmission from target to this point is about 73.7%.
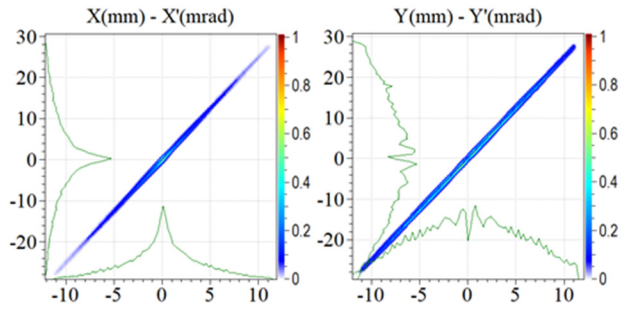

Figure 3: Transverse phase spaces (left: X (horizontal); right: Y (vertical)) at the entrance of the first quadrupole.

At the first quadrupole, hot electrons are deflected due to the external magnetic field. For C^{6+} ions reaching the first quadrupole, the pulse length is approximately 40 ns and the beam current is estimated to be 300 mA. For including of the space charge effect in the following transport line, the three-dimensional PIC method is employed in the simulation.

Energy spread compression is the key issue in the process of beam dynamics design. The ions with initial energy deviation within ±6% are mainly concerned. For the debuncher, the modulated peak voltage of 700 kV, RF frequency of 80 MHz, and transit time factor of 0.85 are adopted. The longitudinal phase spaces upstream and downstream of the debuncher are shown in Fig. 4. By adjusting the amplitude of the RF electric field, the energy spread of the concerned ions (the red circle) can be compressed from ±6% to ±0.6%.
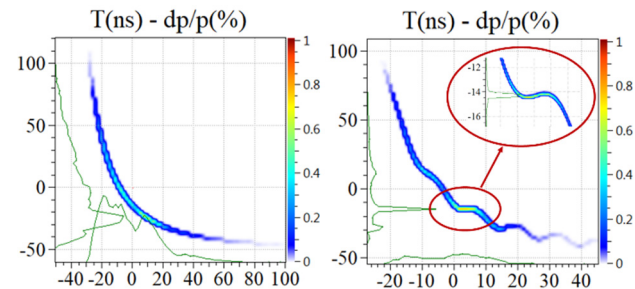

Figure 4: Longitudinal phase spaces upstream (left) and downstream (right) of the debuncher.

To pick out the ions with the energy of within 4 ± 0.024 MeV/u, the 45° bend magnet is adopted for energy selection, of which the pole face rotation angle is 6°, curvature radius is 500 mm and gap distance is 50 mm. As a result of chromatic dispersion of the bend magnet, ions with different energy are dispersed effectively in the horizontal plane.

By regulating the slit width, the proportion of ions within 4 ± 0.024 MeV/u in the total survived ions downstream the slit changes accordingly. The simulation result shows that the proportion can be greater than 95% when the slit width is less than 6 mm.

Taking into consideration the stable beam motion in the synchrotron, the stability is much more sensitive to the emittance in the yy' plane than the xx' plane. For this reason, the effect on particle number and transverse emittances is presented by adjusting the slit height. Figure 5 exhibits the influence of the slit width on output particle number and transverse emittance.

As shown in Fig. 5, when the half width of the slit is 6 mm, as the slit height changes from 0.2 mm to 1.0 mm, the normalized transverse emittances (90%) of the extracted beam at the exit of the injector vary from $2.0\ \pi$ mm·mrad to $3.8\ \pi$ mm·mrad in the xx' plane and $0.1\ \pi$ mm·mrad to $1.0\ \pi$ mm·mrad in the yy' plane, and the output particle number varies from 4.3×10^8 to 1.84×10^9.
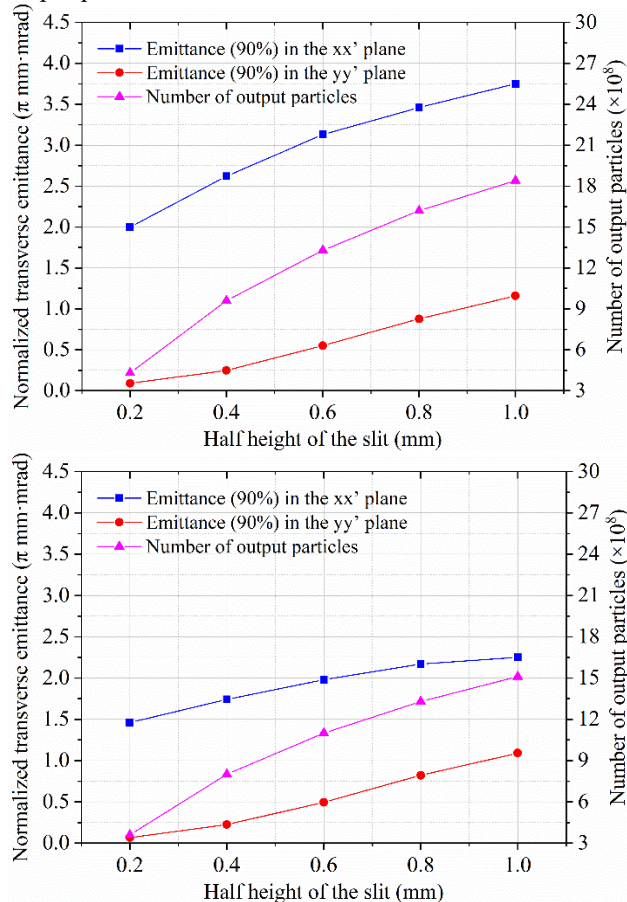

Figure 5: Output particle number and transverse emittances on the half height of the slit. The half width of the slit is 6 mm (top) and 4 mm (bottom).

Moreover, when the slit width is reduced to 4mm, as the slit height changes from 0.2 mm to 1.0 mm, the normalized transverse emittances (90%) vary from $1.5\ \pi$ mm·mrad to $2.3\ \pi$ mm·mrad in the xx' plane and $0.1\ \pi$ mm·mrad to $1.0\ \pi$ mm·mrad in the yy' plane, while the output particle number varies from 3.6×10^8 to 1.51×10^9. It is indicated that the normalized yy' emittance (90%) of the extracted beam at the exit of the injector can be controlled to be less than $1.0\ \pi$ mm·mrad and further decrease is feasible, which is beneficial for the stable beam motion in the synchrotron. The maximum output particle number reaches up to 1.84×10^9 while the maximum normalized xx' emittance (90%) is $3.8\ \pi$ mm·mrad. As the slit height is reduced, the normalized transverse emittances and output particle number decrease.

The RMS transverse envelope of the beam with initial energy spread within ±6% along the longitudinal position in the injector is displayed in Fig. 6.
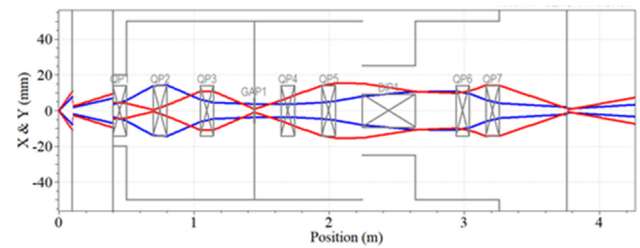

Figure 6: RMS transverse envelope (blue: X; red: Y) along the longitudinal position in the injector (initial energy spread within ±6%).

CONCLUSIONS

To inject laser-accelerated C^{6+} ions into a synchrotron, the beam dynamics design of an injector is carried out. For the reference energy of 4 MeV/u, multiparticle simulation of C^{6+} beam along the injector is developed. It is indicated that the proportion of ions within 4 ± 0.024 MeV/u in the total survived ions of the extracted beam can be larger than 95% when the slit width is less than 6 mm. The normalized yy' emittance (90%) of the extracted beam can be controlled to be less than $1.0\ \pi$ mm·mrad when the slit height is less than 1mm. The maximum output particle number reaches up to 1.84×10^9, and the maximum normalized xx' emittance (90%) is $3.8\ \pi$ mm·mrad, with the slit width of 6 mm and slit height of 1 mm.

REFERENCES

[1] J. G. Zhu *et al.*, "Experimental demonstration of a laser proton accelerator with accurate beam control through image-relaying transport", *Phys. Rev. Accel. Beams*, vol. 22, p. 061302, Jun. 2019.
doi:10.1103/PhysRevAccelBeams.22.061302

[2] E. Noda *et al.*, "Direct injection of laser-accelerated ions into a superconducting synchrotron", in *Proc. 17th Annual Meeting of Particle Accelerator Society of Japan (PASJ'20)*, Online, Sep. 2020, pp. 693-697.

[3] S. Busold *et al.*, "Shaping laser accelerated ions for future applications-The LIGHT collaboration", *Nucl. Instrum. Methods*, vol. 740, pp. 94-98, 2014.
doi:10.1016/j.nima.2013.10.025

[4] S. Yaramyshev, W. Barth, A. Orzhekhovskaya, and B. Zielbauer, "Capture and transport of the laser-accelerated ion beams for the LIGHT project", in *Proc. IPAC'11*, San Sebastián, Spain, Sep. 2011, paper MOODB03, pp. 59-61.

[5] J. Ding *et al.*, "Simulation studies on generation, handling and transport of laser-accelerated carbon ions", *Nucl. Instrum. Methods*, vol. 909, pp. 168-172, 2018.
doi:10.1016/j.nima.2018.02.103

[6] H. Daido *et al*., "Review of laser-driven ion sources and their applications", *Rep. Prog. Phys*, vol. 75, p. 056401, Apr. 2012. doi:10.1088/0034-4885/75/5/056401

[7] S. Palaniyappan *et al.*, "Efficient quasi-monoenergetic ion beams from laser-driven relativistic plasmas", *Nature Communications*, vol. 6, p. 10170, Dec. 2015.
doi:10.1038/ncomms1017

[8] Y. Wan, private communication, Sep. 2020.

[9] F. Nürnberg *et al.*, "Warp simulations for capture and control of laser-accelerated proton beams", *J. Phys.: Conf. Ser.*, vol. 244, p. 022052, 2010.
doi:10.1088/1742-6596/244/2/022052

[10] *Tracewin documentation*, D. Uriot and N. Pichoff, CEA Saclay, May 2020, p. 1-216,
http://irfu.cea.fr/dacm/
logiciels/codesdacm/tracewin/tracewin.pdf